Water Science & Technology

IWA PUBLISHING

Water Science & Technology Vol 85 No 9, 2682 doi: 10.2166/wst.2022.118

Treatment on thiodicarb in pesticide wastewater with walnut shells-derived carbon and its improved modification: adsorption behavior

Haifeng Bai, Bin Wang, Dilinuer Talifu*, Abulikemu Abulizi and Mailikezhati Maihemuti

Key Laboratory of Coal Conversion & Chemical Engineering Process (Xinjiang Uyghur Autonomous Region), School of Chemical Engineering and Technology, Xinjiang University, Urumqi 830046, PR China
*Corresponding author. E-mail: dilnurt@xju.edu.cn

ABSTRACT

The health problems caused by water pollution cannot be ignored, and the contribution of pesticides to water pollution has also become increasingly unignorable. The modified semi-coke as an adsorbent for reducing pesticide pollution to water was obtained from activated semi-coke which was modified by nitric acid (HNO_3). The semi-coke was obtained by carbonization using 60 mesh walnut shell powder. After acid–base deashing, the semi-coke is dipped into zinc chloride ($ZnCl_2$) solution to obtain activated semi-coke. Through BET analysis, the specific surface areas of semi-coke, activated semi-coke and modified semi-coke were 26.8 m^2/g, 243.9 m^2/g, and 339.6 m^2/g respectively. An extremely high adsorption capacity of the adsorbents which is used to treat wastewater was achieved. The optimum adsorption conditions for modified semi-coke on thiodicarb solution were 30 mg/L of thiodicarb solution, adsorbent dosage of 0.01 g, adsorption temperature of 25 °C and adsorption time of 90 min. The optimum adsorption amount of 29.54 mg/gsor was achieved (sor is the abbreviation for sorbent). Moreover, through kinetics study, the result manifests that the modified semi-coke adsorption process is more fitted to the second-order kinetic model. This study provided a research implication theoretically for the treatment of pesticides in water.

Key words: adsorption, biomass semi-coke, kinetic, thiodicarb, walnut shells

HIGHLIGHT

- Constructive methods of activation, modification to improve adsorption behavior of semi-coke is provided. A maximum 339.6 m^2/g surface area is achieved. Isotherm and kinetic studies are investigated. A solution is provided for thiodicarb pesticide treatment in water.

GRAPHICAL ABSTRACT

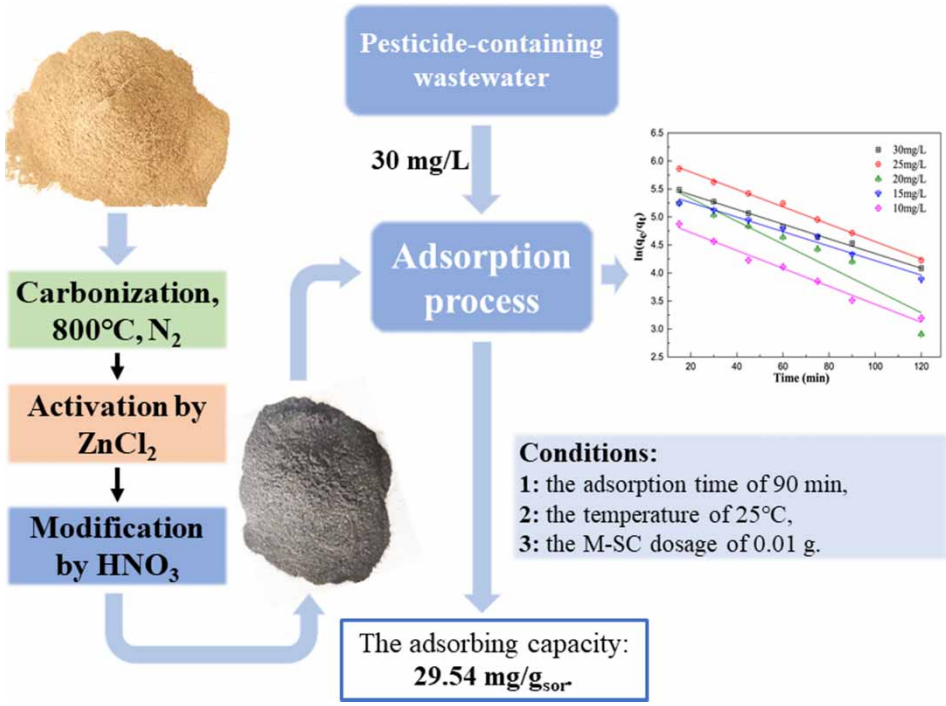

INTRODUCTION

Thiodicarb as an emerging contaminant is one of the most extensively consumed pesticides that constitutes a generation of high-efficiency, broad-spectrum, low-toxicity, systemic carbamate insecticide. It is widely used to eliminate the pests of cotton, vegetables, fruit trees, tea, tobacco, forests, wheat, and other crops, and to control the larvae of Lepidoptera, Homoptera, Hymenoptera, Diptera, Coleoptera, and other pests particularly effective (Akhtar *et al.* 2021). The thiodicarb is currently an excellent agent for controlling resistant cotton bollworm in China which is a major crop planting area that uses pesticides of 0.8 million tons every year and it is repeatedly detected in natural water bodies resulting in water security and water crisis issues. Although thiodicarb is one of the low-toxic derivatives of methomyl, in which the toxicity is greatly weakened, the accumulative effect of pesticides is still non-negligible (Katagi 2010). Hence, the development of high efficiency and economical technologies for thiodicarb removal from wastewater is of prime significance.

To date, many methods have been studied for the removal of contaminants in water such as heavy metal ions (Shi *et al.* 2021), antibiotics, dye (Darwesh *et al.* 2021), endocrine, pesticides (Erol *et al.* 2019), including adsorption (Zeng *et al.* 2019), biodegradation, photo-degradation (Wang *et al.* 2017), and oxidative degradation (Xu *et al.* 2019). Among these methods, adsorption has been recognized as a preferable method to eliminate the pollutants from aqueous solutions due to easy operation, economical cost, high treatment efficiency, and less or no toxic residue generation.

Adsorbents are crucial in the adsorption process. In previous research, many types of adsorbents have been used for removing pesticides, such as carbon-based materials (biochar, activated carbon, carbon nanotube, and graphene) (Xiang *et al.* 2019), clay minerals (Liu *et al.* 2017a), mesoporous silica (Zhang *et al.* 2018), metal–organic frameworks (MOFs) (Jin *et al.* 2019). Zhao *et al.* (2018) achieved adsorption capacity of 6.67–10.34 mg/g for removing the pesticide imidacloprid from aqueous solution by biochar derived from peanut shell. Ranjbar Bandforuzi & Hadjmohammadi (2019) achieved adsorption capacity of 16.58 mg/g when removing the pesticide from aqueous solution using magnetic chitosan nanoparticles. Biomass, due to its low price, easy accessibility, and wide availability, is an optimal selection to be used for producing adsorbents. The unique geographical advantage in western China renders waste biomass resources such as walnut shells abundant. Recycling waste walnut shells can reduce pesticide pollution, conversely, protecting the environment

by decreasing waste disposal or direct combustion emission. However, the internal adsorbing properties of biomass is low. Therefore, a method of modification to process biomass for the aim of higher adsorption capacity is necessary.

However, to the best of our knowledge, work related to $ZnCl_2$ activation and HNO_3 modification of semi-coke (SC) of application for thiodicarb removal has not been reported within the literature. Thereby, considering mostly possible factors, in this study, we choose $ZnCl_2$ as an activator and HNO_3 as a modifier to obtain sorbing material and study the adsorptive properties of thiodicarb. Meantime, we investigated the optimum adsorption conditions. The main works of this study were: (1) synthesis and characterization of SC, activated semi-coke (A-SC), and modified semi-coke (M-SC); (2) study of thiodicarb adsorption behavior on modified semi-coke, including adsorption kinetics, isotherms, and the factors affecting the amount of adsorption.

MATERIALS AND METHODS

Materials and reagents

The walnut shells were purchased from the local market and thiodicarb was purchased from Shanghai Jingchun Biochemical Technology Co., Ltd. NaOH, H_2SO_4 and $ZnCl_2$ were purchased from Hongyan Chemical Reagent Factory, Shengsen Fine Chemical Co., Ltd, and Bodi Chemical Co., Ltd respectively in Tianjin China. HNO_3 and HCl (Guaranteed reagent) were purchased from Tianjin Third Chemical Reagent Factory. The reagents used in this study were of analytical grade except for special instructions.

Preparation of SC

The 60-mesh walnut shell powder (MWSP) was obtained from walnut shells, which were smashed, sieved, washed with deionized water at least three times, and dried at 80 °C overnight. Then, under the conditions of 800 °C, N_2 atmosphere, MWSP were placed in a tube furnace, being pyrolyzed for 120 min with a heating rate of 10 °C. The semi-coke was obtained when the temperature was cooled to room temperature.

Deashing experiment

In the process of preparing semi-coke, some inorganic salts in biomass were converted into ash. The ash will block the pores of semi-coke and affect the adsorption capacity, because this is unfavorable for adsorption. Therefore, the de-ashing process of semi-coke is essential to being an adsorbent. Due to the possible existence of matter, acids and bases can be used to get rid of it. And the main reaction equation could be shown below:

$$SiO_2\ (s) + 2NaOH\ (l) \rightarrow Na_2SiO_3\ (l) + H_2O\ (l) \quad (1)$$

$$Al_2O_3\ (s) + 2NaOH\ (l) \rightarrow 2NaAlO_2\ (l) + H_2O\ (l) \quad (2)$$

$$Fe_2O_3\ (s) + 6HCl\ (l) \rightarrow 2FeCl_3\ (l) + 3H_2O\ (l) \quad (3)$$

$$CaO\ (s) + 2HCl(l) \rightarrow CaCl_2\ (l) + H_2O\ (l) \quad (4)$$

$$MgO\ (s) + 2HCl\ (l) \rightarrow MgCl_2\ (l) + H_2O\ (l) \quad (5)$$

Deashing using alkali

A certain amount of SC which was measured according to liquid to solid mass ratio of 8: 1 of NaOH solution was fully mixed with NaOH solution (12 wt%), and reacted at a constant temperature (55 °C) in a vibrating shaker for 80 min. Then SC was washed with absolute ethanol and deionized water repeatedly and dried at 80 °C until the mass was consistent.

Deashing using acid

A certain amount of SC which had been processed by alkaline deashing was measured according to the liquid to solid mass ratio of 9: 1 of HCl solution and was fully mixed with HCl solution (5 wt%), and reacted at a constant temperature (55 °C) in a vibrating shaker for 80 minutes. Then materials were washed with absolute ethanol and deionized water repeatedly and dried at 80 °C until the mass was consistent. Then final de-ashing SC (D-SC) was obtained.

Preparation of $ZnCl_2$ activated semi-coke

The orthogonal experimental design was employed to optimize the preparation conditions of A-SC with the objective function of static adsorption capacity to thiodicarb. As is shown in Table S1, different influencing factors are designed.

According to the design conditions in Table S1, a certain amount of D-SC determined by design conditions (the same below) was placed in a crucible. The solution was stirring in a room temperature for a certain period after being added to a certain mass concentration of $ZnCl_2$ solution so that it could completely infiltrate the D-SC. This was dried at 120 °C for a certain period, D-SC was placed in a high-temperature tube furnace with a N_2 atmosphere at a certain temperature for a certain period to obtain A-SC.

Preparation of HNO_3 modified semi-coke

The method of synthesizing M-SC was based on a previous study (Jin *et al.* 2018) and was amended and optimized in this study. A certain A-SC was accurately weighed and mixed with HNO_3 solution at a ratio of 1 g A-SC to 15 mL HNO_3 for 30 min and magnetically stirred. The solution was transferred into a hydrothermal reactor, and reacted at 180 °C for 13 hours and then cooled to room temperature. After being repeatedly washed with deionized water and absolute ethanol until constantly neutral and being dried at 80 °C for 8 hours, acid-modified semi-coke was obtained. This was then kept tightly closed.

Characterization methods

The morphology and structure of the prepared semi-coke were characterized by scanning electron microscopy (SEM, SU-8010, Japan). The elemental analysis was performed using energy dispersive X-ray spectroscopy (EDX, INCA-Oxford, High Wycombe, UK). Brunner–Emmet–Teller measurements (BET, Nova1000e, USA) were used to investigate the specific surface area, pore diameter, pore volume, and N_2 adsorption and desorption isotherm, respectively. X-ray photoelectron spectroscopy (XPS, ESCALAB 250Xi, USA) was conducted and utilized to determine the elemental composition.

Adsorption experiments

Batch adsorption experiments were conducted to examine the removal efficiencies. In addition, to optimize the adsorption conditions of M-SC, the adsorption temperature, the initial concentration of thiodicarb, the dosage of SC, and the adsorption time, orthogonal experiments were designed with each factor at three levels, as shown in Table S2. A certain amount of thiodicarb solution was placed in an Erlenmeyer flask surrounded by a thermostatic oscillator. The pH of the solution was kept constant at 7 by acid and base adjustment. The temperature was kept constant, and the adsorbent was transferred to the Erlenmeyer flask. The samples were extracted from the bottles and filtered using a 0.45-μm filter (PES membrane) and analyzed through UV spectrophotometry (UV-T6 New Century, China) at $\lambda_{max} = 236$ nm.

Moreover, adsorption kinetics experiments were conducted by mixing 0.02 g adsorbents and 100 mL thiodicarb solution with different initial concentrations (10, 15, 20, 25, 30 mg/L), at 25 °C with designated time intervals (from 10 to 120 min). Adsorption isotherm experiments for M-SC were performed by adding 0.02 g adsorbents into 100 mL thiodicarb aqueous solutions with different initial concentrations (10–30 mg/L) and shaking at 2 h at 25 °C.

RESULTS AND DISCUSSION

Characterization methods

SEM and EDX analyses

Surface morphology plays the key role in understanding the interactions between adsorbents and adsorbates. From Figure 1(a), the SEM results show that ash particles can be seen on the SC surface. Compared with de-ashing semi-coke (Figure 1(b)), the ash particles on the surface were almost completely removed through de-ashing using alkali and acid. Figure 1(c) and 1(d) displays that multiple micropores and macropores are present on the surface through SC being activated and modified. This is in line with the BET results that showed an improvement in the surface area and the pore volume. The EDX result of MC is shown in Fig. S1 in Supplementary Information. The result showed that C and O were the main elements in MC accompanied with Zn^{2+} and Cl^-.

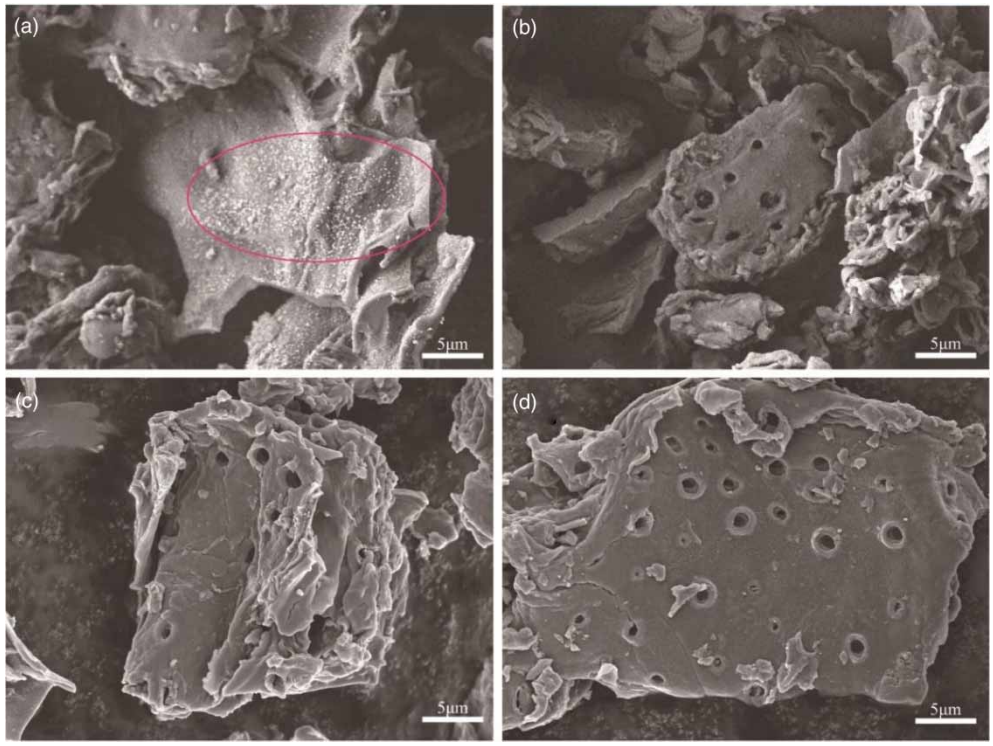

Figure 1 | SEM image of semi-coke (a), de-ashing semi-coke (b), activated semi-coke (c) and modified coke (d).

XRD and XPS analyses

The XRD patterns of SC and M-SC are shown in Figure 2(a). The diffraction peak at 26.6° can be assigned to amorphous carbon (Zhen *et al.* 2019). Compared with SC, the diffraction peaks at 31.6°, 34.3°, 36.1°, 47.4°, 56.5°, 62.7°, and 67.7° (PDF#36-1451) indicate the formation of ZnO in the prepared A-SC from Figure 2(a).

The functional groups on the surface of the material affect its electrochemical performance. By XPS, the surface chemical compositions of SC, A-SC, and M-SC were analyzed. As shown in Figure 2(b), XPS survey spectra are displayed. The samples have three peaks at 284.8, 403.1, and 533.7 eV that are consistent with the characteristic spectra of C 1s, N 1s, and O 1s orbitals, respectively. The peaks at 1,022.7 eV and 1,045.8 eV correspond to Zn $2p_{3/2}$ and Zn $2p_{1/2}$ (Figure 2(c)), further proving the existence of Zn or ZnO on A-SC (Bankar *et al.* 2019). After modification, the Zn content decreased or even disappeared on M-SC, which could be attributed to HNO_3 reacting with metal oxides. The N 1s spectrum of M-SC was fitted to two peaks shown in Figure 2(d). Two peaks at 400.2 eV, 405.9 eV, are assigned to C-NH_2, -NO_3 groups, respectively. The presence of these oxygen-containing and nitrogen-containing functional groups on M-SC can promote good contact between the surface of the material and the adsorbate (Ru *et al.* 2020), thereby enhancing the adsorption capacity of the material.

BET analyses

BET results for SC, A-SC, and M-SC particles are given in Figure 3. The results show that the methods of activation of $ZnCl_2$ and modification of HNO_3 increase the surface area by about 9 and 12 times compared with untreated SC from 26.8 to 243.9 and 339.6 m^2/g. Furthermore, as expected, by activating and modifying the SC, the total pore volume increased from 0.013 to 0.114 and 0.167 cm^3/g, while the average pore diameter reduced from 288.0 to 34.7 and 19.7 Å. This suggests that the process of activation and modification of SC creates new pores within the structure.

In Figure 4(a), pore-size distribution curves of SC, A-SC, and M-SC are depicted. The nitrogen adsorption/desorption isotherms of M-SC are shown in Figure 4(b). The N_2 isotherm of M-SC is a blend of type I isotherms and type H4 hysteresis loop, the sharp increment in the adsorption volume at extremely low relative pressure demonstrated the microporous textural properties which is a typical characterization of activated carbon. The distribution of pore width based on the

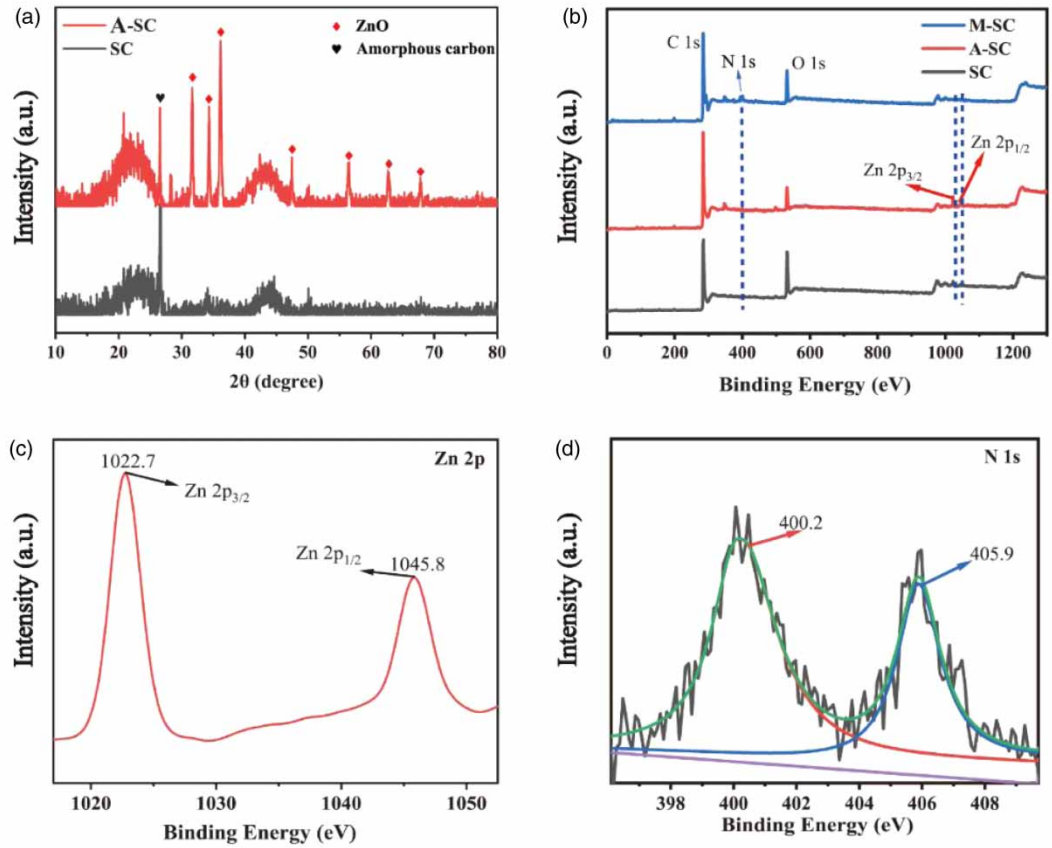

Figure 2 | (a) XRD, (b) XPS survey spectra, (c) high-resolution XPS Zn 2p spectrum of A-SC, (d) high-resolution XPS N 1s spectra.

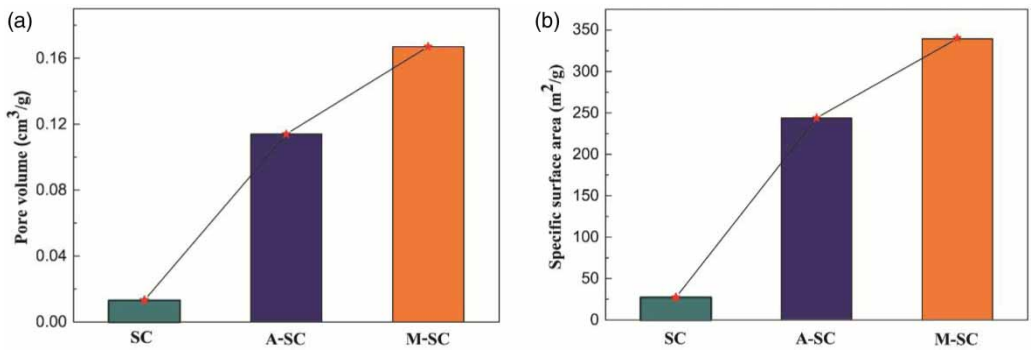

Figure 3 | Pore volume (a) and specific surface area (b) of SC, A-SC, and M-SC.

Barrett–Joyner–Halenda indicates that the average pore width is about 1.968 nm. It depicts the existence of micropores and macropores of 1–5 nm and 20–200 nm, respectively.

Adsorption results

Optimization of preparation of A-SC

According to designed conditions of influencing factors and level values, nine types of A-SC were prepared. The adsorption experiments were conducted on the initial concentration of 10 mg/L and volume of 40 mL of thiodicarb. The adsorption temperature was 25 °C, the contact time is 120 min, the dosage of A-SC is 0.1 g. The adsorption results of nine types of

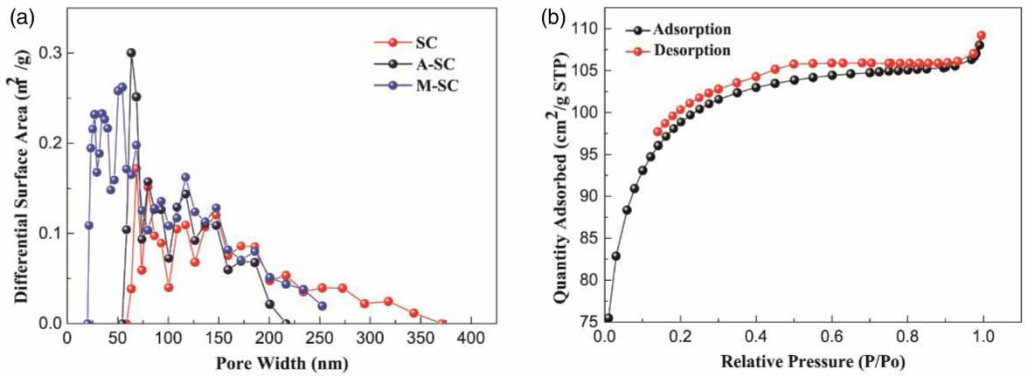

Figure 4 | (a) Pore-size distribution curve of SC, A-SC, and M-SC. (b) Nitrogen adsorption/desorption isotherms of M-SC.

Table 1 | Optimization results of preparation of A-SC and range analysis results

	Activator concentration (%)	Impregnation time (h)	Activation temperature (°C)	Activation time (min)	Adsorption capacity to thiodicarb (mg/g)
1	10	12	400	90	1.86
2	10	24	500	120	1.79
3	10	36	600	150	2.00
4	15	12	500	150	2.19
5	15	24	600	90	1.96
6	15	36	400	120	1.54
7	20	12	600	120	1.91
8	20	24	400	150	1.59
9	20	36	500	90	1.76
K_1	5.65	5.97	5.00	5.58	
K_2	5.69	5.34	5.74	5.24	
K_3	5.27	5.30	5.87	5.78	
R	0.14	0.22	0.29	0.18	

A-SC and the range analysis results show in Table 1. Only considering the condition of maximum adsorbing capacity, by the K factors, the optimum preparation conditions of A-SC are $ZnCl_2$ concentration of 15%, soaking time of 12 h, activation temperature of 600 °C, and activation time of 150 min. To investigate the accuracy of design results, an adsorption experiment was conducted with the optimum preparation conditions and the result showed that the adsorbing capacity to thiodicarb was 2.47 mg/g_{sor} which was the highest. Hence it was confirmed. In addition, through range analysis from Table 1, the influence of several factors on the adsorption performance of A-SC adsorbing thiodicarb is activation temperature > soaking time > activation time > activator concentration.

Optimization of adsorption conditions of M-SC

To evaluate the effects of the initial target molecule concentration, temperature, time, and dosage of M-SC, as was shown in Table S2, three levels for each factor were designed and the results are shown in Table 2. The influence of several factors on the adsorption performance of thiodicarb for M-SC is adsorption temperature > M-SC dosage > initial concentration of thiodicarb > adsorption time by range analysis. Through the K factor in Table S3, the best adsorption conditions are the initial concentration of thiodicarb of 30 mg/L, the adsorption time of 90 min, the temperature of 25 °C, and the M-SC dosage of 0.01 g. To investigate the accuracy of design results, an adsorption experiment was conducted with the optimum adsorption conditions and the result showed that the adsorbing capacity to thiodicarb was 29.54 mg/g_{sor}.

Table 2 | The adsorption experimental results of M-SC

	Adsorption temperature (°C)	The initial concentration of thiodicarb (mg/L)	Dosage of carbo-coal (mg)	Adsorption time (min)	Adsorption capacity to thiodicarb (mg/g)
1	0	20	0.01	30	21.48
2	0	30	0.02	60	20.65
3	0	40	0.03	90	19.14
4	25	20	0.02	90	25.00
5	25	30	0.03	30	25.00
6	25	40	0.01	60	28.89
7	50	20	0.03	60	16.67
8	50	30	0.01	90	29.41
9	50	40	0.02	30	17.43

Adsorption kinetics

To evaluate the adsorption kinetics behaviors of thiodicarb by M-SC, the models of pseudo-first order and pseudo-second order were used to fit experimental data. The equations of these models are presented in Table S4.

Figure 5 presents the nonlinear-fitting results of pseudo-second order and pseudo-first order models and Table 3 shows the kinetics parameters. At different initial concentrations, the correlation coefficient R^2 of the pseudo-second order model was always higher than the pseudo-first order model and the nonlinear fitting curves of the pseudo-second order model were always much more close to the experimental data points than the pseudo-

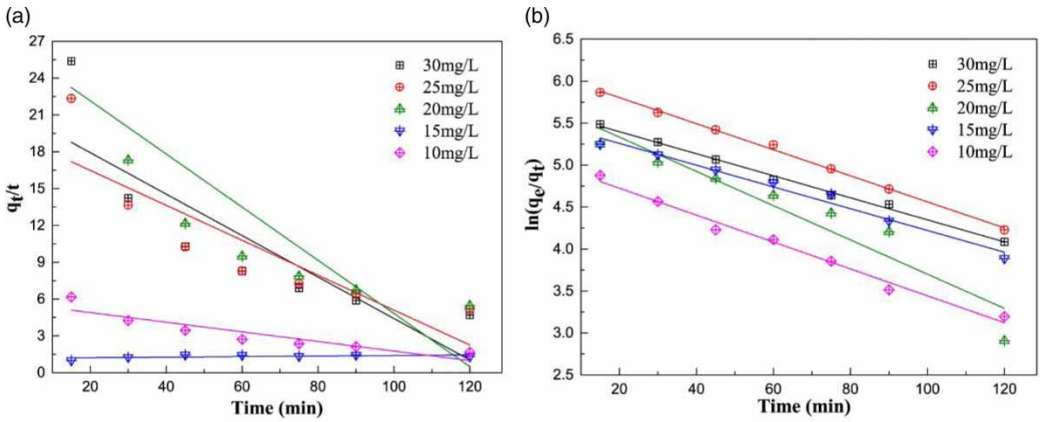

Figure 5 | Kinetics of thiodicarb adsorption onto M-SC by fitting the pseudo-second order (a) and pseudo-first order model (b).

Table 3 | Parameters of the pseudo-second order and pseudo-first order kinetic models of thiodicarb adsorption onto M-SC

	Pseudo-second order		Pseudo-first order	
C_0 (mg/L)	k_2 (g/mg/min)	R^2	k_1 (min^{-1})	R^2
10	−0.013	0.983	−0.169	0.797
15	−0.016	0.977	−0.142	0.113
20	−0.020	0.885	−0.217	0.645
25	−0.013	0.997	0.002	0.704
30	−0.016	0.994	−0.039	0.672

second order model could better describe adsorption kinetics, which implicated that the adsorption of thiodicarb by M-SC has been involved with chemisorption (Liu *et al.* 2017b).

Adsorption isotherms

Langmuir's model presumes that the adsorbent has homogenous sites, and the adsorption is monolayer, in which there are no interactions between molecules and adsorbent. The experimental data were not well fitted by Langmuir model with the low correlation coefficients from Figure 6(a). Freundlich isotherm describes the imperfect and reversible adsorption, concerning formation of the multilayer over the adsorbent with non-uniform distribution of adsorption heat and affinities over the heterogeneous surface (Adamson & Gast 1967). The experimental data were well fitted by the Freundlich model (Figure 6(b)), indicating that physical adsorption existed on the surface of M-SC. The kinetic data had shown the existence of chemisorption. Hence, the multiple actions containing chemisorption and physical adsorption existed in the adsorption process.

Thermodynamic analysis

To determine the effect of temperature on M-SC adsorption, the range of 313, 318, 323 K were studied. As shown in Table 4, positive values of ΔH indicated that the adsorption processes are endothermic, which suggests favorable reactions at high temperatures. Positive ΔS values indicated that the favorable adsorption stability made the adsorption process irreversible and increased the randomness of the solid–liquid interface. The ΔG value increases with increasing temperature, indicating that a favorable reaction is achieved at high temperatures. However, a negative ΔG indicates that the adsorption is spontaneous. Furthermore, ΔG values in the range of −20 to 0 kJ/mol indicate the nature of physical adsorption (Feng *et al.* 2011), which is supported by the R^2 value of the Freundlich isotherm.

A comparison between different pesticides adsorbents

As shown in Table 5, Zhao *et al.* (2018) reported the 6.67–10.34 mg/g adsorption capacity of the imidacloprid removal by biochar. Damdib *et al.* (2019) reported 34.23 mg/g as maximum adsorption capacity during paraquat removal by magnetic biochar. Suo *et al.* (2019) reported 79.55 mg/g as maximum adsorption capacity during triazine removal by modified biochar. The maximum adsorption capacity of 29.54 mg/g was achieved in this study. Compared with other studies, this study provided a competitive and promising methods for pesticide wastewater treatment.

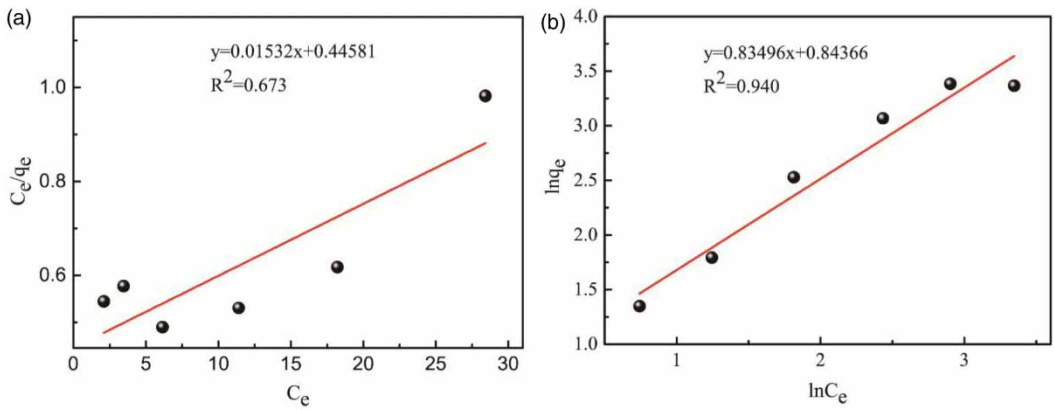

Figure 6 | Linear Langmuir adsorption (a) and Freundlich adsorption (b) isotherm plot for thiodicarb adsorption using M-SC.

Table 4 | Thermodynamic parameters

C_0 (mg/L)	T (K)	K_d	ΔG (kJ/mol)	ΔH (kJ/mol)	ΔS (J/mol·k)	R^2
30	313	1.02	−2.65	179.5	578	0.989
	318	1.21	−3.15			
	323	2.32	−6.04			

Table 5 | Pesticides removal by adsorption methods

Adsorbate	Adsorbent	Adsorption capacity (mg/g)	References
Imidacloprid	Biochar	6.67–10.34	Zhao *et al.* (2018)
Paraquat	Magnetic biochar	34.23	Damdib *et al.* (2019)
Triazine	Modified biochar	79.55	Suo *et al.* (2019)
Thiodicarb	MC	29.54	This study

Recycle performance

As for an adsorbent, the regeneration and reusability capacities are the critical parameters to assess the large-scale application. The recycling efficiency of the selected sorbent is 81.2%. After five adsorption–desorption cycles, the adsorption capacities of M-SC for thiodicarb decreased from 29.5 mg/g to 21.2 mg/g. The result indicates that M-SC possesses an acceptable capacity of regeneration and reusability, which can be used as a promising adsorbent for thiodicarb wastewater treatment. Looking from the other side, recycling performance revealed that it is physical adsorption dominates in processes with chemisorption enhancing adsorption capacity.

CONCLUSION

This study demonstrated the utilization of waste nut walnut shells for water body remediation in aqueous solutions. Methods of activation, modification improved adsorption behavior of semi-coke by walnut shells for thiodicarb from 2.47 mg/g_{sor} to 29.54 mg/g_{sor} in aqueous solution, with a surface area of about 9 and 12 times compared with SC from 26.8 to 243.9 and 339.6 m^2/g. Large specific surface areas and abundant surface functional groups enhance the adsorption capacity of M-SC. Further, the pseudo-second order kinetic model was the most suitable to describe the data obtained experimentally. Isotherm and kinetic studies were performed to characterize the adsorption process, which evaluates the quick and efficient chemical adsorption process. As a result, the HNO_3 modification following activation by $ZnCl_2$ into a semi-coke resulted in a superior adsorbent with promising adsorption and kinetic features and was classified as an alternative adsorbent for future studies. Modified semi-coke obtained by activation and modification of walnut shell provides an effective adsorbent for treating pesticides in wastewater.

ACKNOWLEDGEMENTS

This work was supported by the National Natural Science Foundation of China (No. 41967050).

CONFLICTS OF INTEREST

No.

DATA AVAILABILITY STATEMENT

All relevant data are included in the paper or its Supplementary Information.

REFERENCES

Adamson, A. W. & Gast, A. P. 1967 *Physical Chemistry of Surfaces*. Interscience Publishers, New York.

Akhtar, Z. R., Tariq, K., Handler, A. M., Ali, A., Ullah, F., Ali, F., Zang, L. S., Gulzar, A. & Ali, S. 2021 Toxicological risk assessment of some commonly used insecticides on Cotesia flavipes, a larval parasitoid of the spotted stem borer Chilo partellus. *Ecotoxicology* **30**, 448–458.

Bankar, D. B., Hawaldar, R. R., Arbuj, S. S., Moulavi, M. H., Shinde, S. T., Takle, S. P., Shinde, M. D., Amalnerkar, D. P. & Kanade, K. G. 2019 $ZnCl_2$ loaded TiO_2 nanomaterial: An efficient green catalyst to one-pot solvent-free synthesis of propargylamines. *RSC Advances* **9**, 32735–32743.

Damdib, S., Phamornpiboon, P., Siyasukh, A., Thanachayanont, C., Punyapalakul, P. & Tonanon, N. 2019 Paraquat pesticide removal by magnetic biochar derived from corn husk. In *The 2019 Pure and Applied Chemistry International Conference*.

Darwesh, O. M., Abd El-Latief, A. H., Abuarab, M. E. & Kasem, M. A. 2021 Enhancing the efficiency of some agricultural wastes as low-cost absorbents to remove textile dyes from their contaminated solutions. *Biomass Conversion and Biorefinery* **11**, 1–2.

Erol, K., Yıldız, E., Alacabey, İ., Karabörk, M. & Uzun, L. 2019 Magnetic diatomite for pesticide removal from aqueous solution via hydrophobic interactions. *Environmental Science and Pollution Research* **26**, 33631–33641.

Feng, Y., Yang, F., Wang, Y., Ma, L., Wu, Y., Kerr, P. G. & Yang, L. 2011 Basic dye adsorption onto an agro-based waste material – sesame hull (*Sesamum indicum* L.). *Bioresource Technology* **102**, 10280–10285.

Jin, J., Li, S., Peng, X., Liu, W., Zhang, C., Yang, Y., Han, L., Du, Z., Sun, K. & Wang, X. 2018 HNO_3 modified biochars for uranium (VI) removal from aqueous solution. *Bioresource Technology* **256**, 247–253.

Jin, J., Yang, Z., Xiong, W., Zhou, Y., Xu, R., Zhang, Y., Cao, J., Li, X. & Zhou, C. 2019 Cu and Co nanoparticles co-doped MIL-101 as a novel adsorbent for efficient removal of tetracycline from aqueous solutions. *Science of The Total Environment* **650**, 408–418.

Katagi, T. 2010 Bioconcentration, bioaccumulation, and metabolism of pesticides in aquatic organisms. *Reviews of Environmental Contamination and Toxicology* **204**, 1–132.

Liu, S., Wu, P., Yu, L., Li, L., Gong, B., Zhu, N., Dang, Z. & Yang, C. 2017a Preparation and characterization of organo-vermiculite based on phosphatidylcholine and adsorption of two typical antibiotics. *Applied Clay Science* **137**, 160–167.

Liu, S., Xu, W. H., Liu, Y. G., Tan, X. F., Zeng, G. M., Li, X., Liang, J., Zhou, Z., Yan, Z. L. & Cai, X. X. 2017b Facile synthesis of Cu(II) impregnated biochar with enhanced adsorption activity for the removal of doxycycline hydrochloride from water. *Science of the Total Environment* **592**, 546–553.

Ranjbar Bandforuzi, S. & Hadjmohammadi, M. R. 2019 Modified magnetic chitosan nanoparticles based on mixed hemimicelle of sodium dodecyl sulfate for enhanced removal and trace determination of three organophosphorus pesticides from natural waters. *Analytica Chimica Acta* **1078**, 90–100.

Ru, S., Wang, X., Ma, G., Tan, J., Xiao, H. & Ai, Z. 2020 Facile fabrication of graphitization-enhanced wrinkled paper-like N-doped porous carbon via a ZnCl2-modified NaCl-template method for use as an anode in lithium ion batteries. *Sustainable Energy and Fuels* **4**, 3477–3486.

Shi, X., Mai, X., Wei, R., Ma, Y., Naik, N., He, Z., Chen, Y., Wang, C., Dong, B. & Guo, Z. 2021 Removing Pb^{2+} and As(V) from polluted water by highly reusable Fe-Mg metal–organic complex adsorbent. *Powder Technology* **383**, 104–114.

Suo, F., You, X., Ma, Y. & Li, Y. 2019 Rapid removal of triazine pesticides by P doped biochar and the adsorption mechanism. *Chemosphere* **235**, 918–925.

Wang, W., Fang, J., Shao, S., Lai, M. & Lu, C. 2017 Compact and uniform TiO_2@ g-C_3N_4 core-shell quantum heterojunction for photocatalytic degradation of tetracycline antibiotics. *Applied Catalysis B* **217**, 57–64.

Xiang, Y., Xu, Z., Wei, Y., Zhou, Y., Yang, X., Yang, Y., Yang, J., Zhang, J., Luo, L. & Zhou, Z. 2019 Carbon-based materials as adsorbent for antibiotics removal: mechanisms and influencing factors. *Journal of Environmental Management* **237**, 128–138.

Xu, L., Dong, H., Xu, K., Li, J. & Qiang, Z. 2019 Accelerated degradation of pesticide by permanganate oxidation: a comparison of organic and inorganic activations. *Chemical Engineering Journal* **369**, 1119–1128.

Zeng, Z., Ye, S., Wu, H., Xiao, R., Zeng, G., Liang, J., Zhang, C., Yu, J., Fang, Y. & Song, B. 2019 Research on the sustainable efficacy of g-MoS_2 decorated biochar nanocomposites for removing tetracycline hydrochloride from antibiotic-polluted aqueous solution. *Science of the Total Environment* **648**, 206–217.

Zhang, Z., Li, H. & Liu, H. 2018 Insight into the adsorption of tetracycline onto amino and amino–Fe^{3+} gunctionalized mesoporous silica: Effect of functionalized groups. *Journal of Environmental Sciences* **65**, 171–178.

Zhao, R., Ma, X., Xu, J. & Zhang, Q. 2018 Removal of the pesticide Imidacloprid from aqueous solution by biochar derived from peanut shell. *BioResources* **13**, 5656–5669.

Zhen, H., Wang, H. & Xu, X. 2019 Preparation of porous carbon nanofibers with remarkable microwave absorption performance through electrospinning. *Materials Letters* **249**, 210–213.

First received 3 March 2022; accepted in revised form 25 March 2022. Available online 7 April 2022